An Efficient Method Based on Lattice Construction and the Genetic Algorithm for Optimization of Large Lennard-Jones Clusters

Yuhong Xiang, Haiyan Jiang, Wensheng Cai, and Xueguang Shao*

Department of Chemistry, University of Science and Technology of China, Hefei, Anhui, 230026, P. R. China

Received: December 10, 2003; In Final Form: February 11, 2004

Geometric methods for the construction of three structural motifs, the icosahedron, Ino's decahedron, and the complete octahedron, are proposed. On the basis of the constructed lattices and the genetic algorithm, a method for optimization of large size Lennard-Jones (LJ) clusters is presented. Initially, the proposed method is validated by optimization of LJ_{13-309} clusters with the above structural motifs. Results show that the proposed method successfully located all the lowest known minima with an excellent performance; for example, based on Ino's decahedron with 147 lattice sites, the mean time consumed for successful optimization of LJ_{75} is only 0.61 s (Pentium III, 1 GHz), and the percentage success is 100%. Then, putative global minima of $LJ_{310-561}$ clusters are predicted with the method. By theoretical analysis, these global minima are reasonable, although further verification or proof is still needed.

1. Introduction

Atomic clusters, that is, aggregates of a few to tens of thousands of atoms, are investigated increasingly because they provide a bridge between an atom and the bulk material. In the research of atomic or molecular clusters, the geometric structure with the lowest energy and the dependence of structure on cluster size are particularly complex and intriguing issues. The most stable structure of a cluster is often the geometry with the lowest potential energy. Unfortunately, the task of minimizing the energy of a cluster is notoriously difficult because the number of local minima tends to grow exponentially with cluster size N.[1] For example, when the cluster size is 13, there are at least 988 minima. However, in the case of $N = 100$ there are more than 10^{140} minima.[2] Therefore, finding the global minimum is a nontrivial (in fact, an NP-hard) problem.

Different algorithms have been applied to solve the global optimization problem, such as the genetic algorithm (GA),[3−5] simulated annealing (SA),[6−10] basin-hopping,[11] the fast annealing evolutionary algorithm (FAEA)[12,13], and the random tunneling algorithm (RTA).[14] Good results have been obtained by the above algorithms for small clusters with atoms less than 116. Nevertheless, when the size of the cluster is large, the problem of optimization of clusters only by search strategies is not fully solved.

The modeling method makes the energetic study easier, which is the reason that it is often used to assess the relative energetic merits of various structural motifs and their dependence on cluster size. Such investigations have been employed in a variety of cluster systems including rare gas clusters,[15−17] nickel clusters,[18] iron clusters,[19] C60 molecular clusters,[20] calcium and strontium clusters,[21] and so forth. Furthermore, applications of the modeling method in the optimization of clusters have also been reported;[22−24] for example, Northby[22] and Romero[24] had successfully investigated the optimal structures of LJ_{13-147} and $LJ_{148-309}$ clusters, respectively.

For Lennard-Jones (LJ) clusters, Farges[15] concluded that, when the size is less than 1600, the stable structures belong to the icosahedral sequence, but when the size nears the magic numbers of a decahedron or octahedron, their energies may be lower than that of icosahedral structures. For example, the global optimal structures of LJ_{38} and LJ_{75} are the truncated octahedron and Marks' decahedron, respectively. All the known structures of Lennard-Jones clusters in the range $13 \leq N \leq 309$ belong to the above structural motifs except for the truncated tetrahedron of the LJ_{98} cluster. However, the truncated tetrahedron is not energetically competitive for large Lennard-Jones clusters, because it is not sufficiently spherical.[25]

Geometric construction methods for three structural motifs, the icosahedron, Ino's decahedron, and the complete octahedron, are proposed. In addition, an algorithm for optimization of large size clusters is developed based on the constructed lattice and the genetic algorithm. By optimization of LJ_{13-309} clusters with the three structural motifs, it is found that the proposed method successfully located all the lowest known minima with an excellent performance. Furthermore, putative global minima of Lennard-Jones clusters in the range $309 < N \leq 561$ are predicted with the method. The results indicate that all the clusters are icosahedral motifs, and the structures with an incomplete core occupy a high proportion. Moreover, the proportion of FC (anti-Mackay icosahedron) configurations in the range $309 < N \leq 561$ is low.

2. Method

2.1. Lattice Construction. The structural motifs of Lennard-Jones clusters include the icosahedron, Marks' decahedron, the truncated octahedron, and the truncated tetrahedron. However, because the truncated tetrahedron is not energetically competitive for large size clusters,[25] the tetrahedral lattice is not constructed in this work. Marks' decahedron can be derived from Ino's decahedron by notching the sites at the five twinned boundaries, and the truncated octahedron can be obtained by symmetrically truncating some sites at the six vertices from its complete structure. Therefore, geometric methods for the construction of the icosahedron, Ino's decahedron, and the complete octahedron are proposed to study large size clusters.

Ino's decahedron is a multishell structure, and each shell has the same configuration. The inner decahedron, as shown in Figure 1a by the thin solid lines, is a 13-atom core of Ino's

* Corresponding author. Phone: +86-551-3606160. Fax: +86-551-3601592. E-mail: xshao@ustc.edu.cn.

10.1021/jp037780t CCC: $27.50
Published on Web 03/19/2004

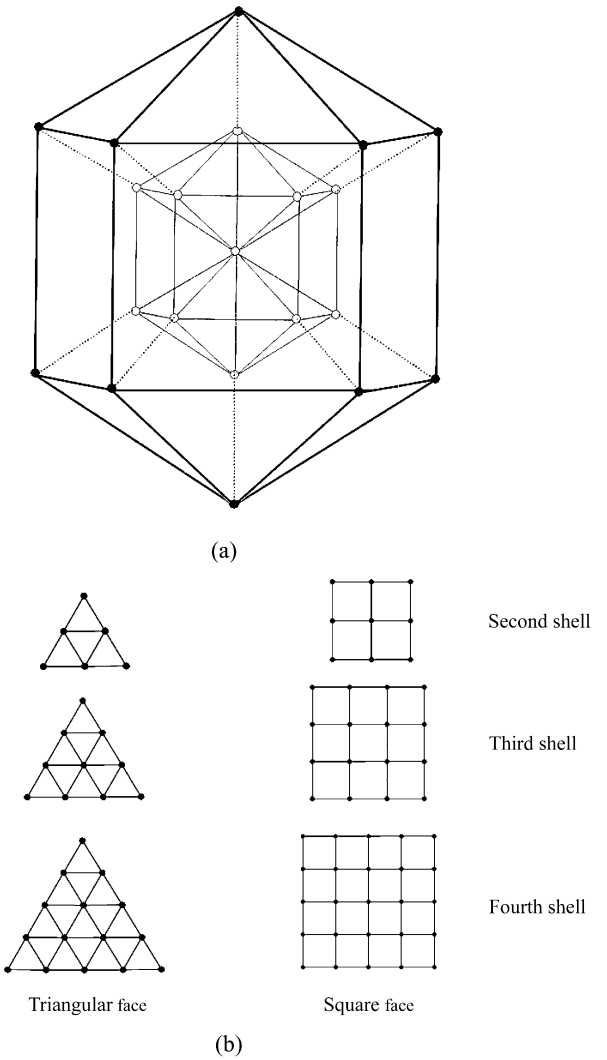

Figure 1. Construction of Ino's decahedron. (a) The construction of vertices, edges, and faces of the second shell. (b) The configurations of the triangular and square faces in different shells.

decahedron, which can be taken from the first decahedral structure of LJ_{75}. The large Ino's decahedron can be constructed from the 13-atom core by the following procedures:

(1) Locate the positions of vertex atoms (lattice sites) of the outer shell. As illustrated in Figure 1a, initially join the central atom with the vertex atoms of the core by lines, then extend them by a length d (d is the distance between the central atom and vertex atom). The ends of the dash lines will determine the positions of the vertex atoms of the outer shell. The positions of the vertex atoms of the nth shell can be determined by further extending the dash lines with length $(n - 1)d$.

(2) Obtain the edges and faces of the outer shell. When the nearest vertices of the same shell are connected, the edges of Ino's decahedron can be obtained. The edges on the same plane will form the triangular and square faces.

(3) Locate the lattice sites on the edges and faces. The lattice sites on the triangular and square faces can be located according to their corresponding configurations, as shown in Figure 1b. The position of each site is defined by the Cartesian coordinates (x,y,z). The values can be calculated according to the coordinates of the 13-atom core. With this method, Ino's decahedra of any size can be constructed.

The icosahedron is also a multishell structure with two models, that is, the Mackay icosahedron (IC) and the anti-Mackay icosahedron (FC). The core of the FC is the same as that of the IC, but atoms on the face of the outermost shell lie in hexagonally close-packed positions relative to the nearest shell of the Mackay icosahedron.[26] The 13-atom core of the icosahedron, as shown in Figure 2a, can be obtained from the known structure of LJ_{13}. The IC and the inner shells of the FC can be constructed using the same method as that used to construct Ino's decahedron. Initially, locate the vertex positions, then, obtain the edges and faces, and finally, locate the lattice sites on the edges and triangular faces according to the corresponding configuration, as shown in Figure 2b. For the outermost shell of the FC, the lattice sites on the faces of the FC unit are located according to the corresponding configuration, as shown in Figure 2b.

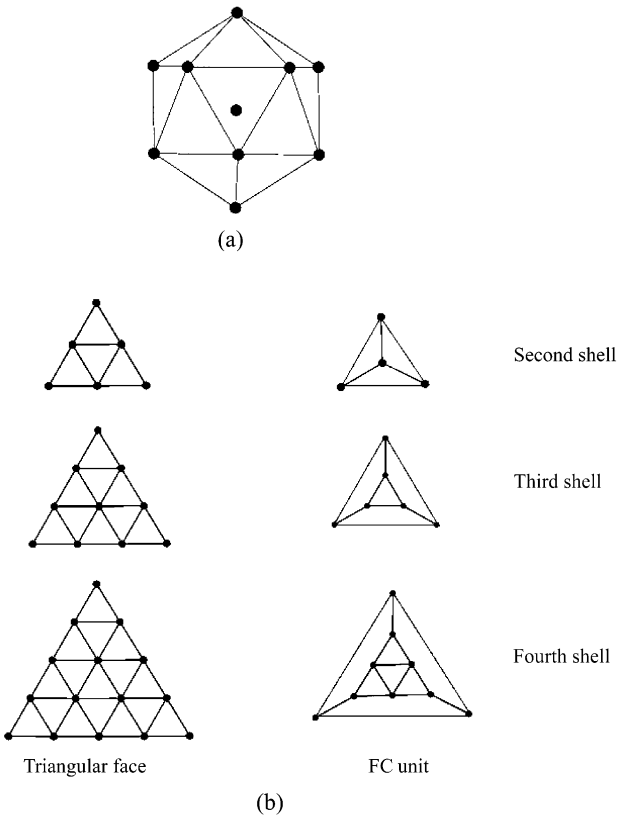

Figure 2. Configuration of the icosahedron. (a) The 13-atom core of the icosahedron. (b) The configurations of the triangular faces and FC units in different shells.

The complete octahedron is constructed with a method similar to that used to construct Marks' decahedron as reported in ref 27. Taking the complete octahedron in Figure 3a as an example, it can be decomposed into five different size squares L_k ($k = 1$, 2, 3, 4, 5), as shown in Figure 3b. Here, L_1 is a special square with one atom. Apparently, the complete octahedron can be constructed by putting each square together according to the layout in Figure 3c. If k atoms locate on the edges of the maximal square, the complete octahedron will have $2k - 1$ squares. To construct the complete octahedron, the squares are arranged in the following order: L_1, L_2, L_3, ..., L_{k-1}, L_k, L_{k-1}, ..., L_3, L_2, L_1. The distance between two nearest atoms and the distance between two squares are taken from the known structure of LJ_{38}.

In order to obtain the optimal lattice with the lowest energy, a limited memory BFGS (L-BFGS) method is performed to optimize the above constructed lattices with the Lennard-Jones pair potential.[28,29]

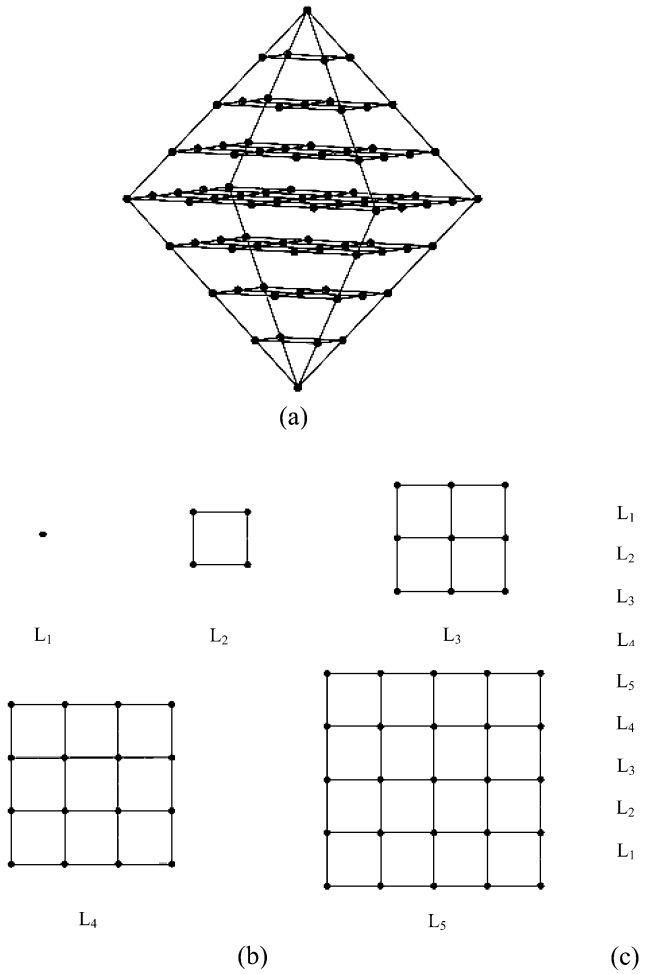

Figure 3. Construction of the complete octahedron. (a) An example of a complete octahedron with 85 atoms. (b) Configurations of different sizes of squares in the complete octahedron. (c) Layout of the complete octahedron.

2.2. Lattice Search with the Genetic Algorithm. Recently, there have been several applications of the genetic algorithm dealing with the problem of obtaining the lowest energy structures of atomic or molecular clusters.[3−5,30−33] The GA is a stochastic global minimization technique, which is inspired by concepts from Darwin's natural evolution theory. Populations of candidate solutions compete with each other for survival. Through selection, crossover, and mutation operations, the fitter individuals pass their characteristics on to the latter generations. In this way, it can be expected that the fittest individual can be obtained after hundreds or thousands of generations. In the case of the structural optimization of clusters, the "fitness" is the absolute value of the potential energy of the corresponding geometric structure, with lower potential having higher fitness. The structure represented by the individual with the highest fitness is the most stable one. The detailed procedures of the lattice search with GA are represented as follows:

(1) Initialization. An initial population with 20 individuals is generated as follows: N atoms are distributed randomly on the constructed lattices including N_s sites. This defines the initial configurations of the Lennard-Jones clusters, which can be represented using gene strings with N_s genes. Each gene corresponds to a lattice site, whose value is 1 if the site is occupied by an atom or 0 if it is not.

(2) Evaluation. At first, Cartesian coordinates of each atom in each structure represented by an individual are obtained according to the gene string. Then, by using these coordinates, the energy can be calculated with the Lennard-Jones pair potential

$$E = 4\epsilon \sum_{i<j} \left[\left(\frac{\sigma}{r_{ij}}\right)^{12} - \left(\frac{\sigma}{r_{ij}}\right)^{6} \right] \quad (1)$$

where r_{ij}, ϵ, and $2^{1/6}\sigma$ are the distance between atoms i and j, the pair well depth, and the equilibrium pair separation, and $\epsilon = \sigma = 1$ with reduced units.

(3) Selection. Individuals that will serve as parents are chosen randomly from the population, where the probability to be chosen is related to its fitness value.

(4) Breeding. The individuals of the next generation are generated by a directed mutation operation. The site occupied by an atom is selected randomly from the set of loosely bound sites that have fewer atoms around them, and the value of the corresponding gene is set to 0. At the same time, a vacant site is selected randomly from the set of tightly bound vacant sites that have more atoms around them, and the value of the corresponding gene is changed to 1. The process is repeated until it reaches a tighter structure. In order to maintain the diversity of population, a relatively high mutation rate of 0.06 is used. On the other hand, the crossover operation as generally used in GAs is not employed because it is difficult to guarantee that the individuals of the next generation contain the correct number of atoms. Therefore, the algorithm used in this work is a simplified GA, instead of a standard GA.

(5) Local Search with L-BFGS. Because of the asymmetry of the outer atoms, the force exerting on the core is not symmetric. Consequently, the positions of atoms may deviate slightly from the lattice sites. Therefore, when a minimum occurs, a limited memory BFGS (L-BFGS) will be performed to obtain the optimal structure of the LJ cluster.

(6) Stopping Criteria. Two termination conditions are used for the known lowest minima. First, the calculation will terminate when the known lowest minimum is found. Second, if the number of iterations exceeds 500, the calculation will stop. However, in the optimization of large Lennard-Jones clusters in the range of $309 < N \leq 561$, only the second termination condition is used.

In general, the growth of icosahedral and decahedral clusters is from the inner to the outer shell; therefore, the lattice sites of icosahedral and decahedral cores can be fixed in the optimization. However, because the exposed vertex atoms are more unstable than the atoms on faces of the outermost shell as a result of fewer neighbors, the structures with an incomplete core might be good candidates for LJ clusters.[34] Therefore, the 12 vertex sites of the inner icosahedron are not fixed. For the decahedron, Marks' decahedron can be derived by notching a different number of atoms from Ino's decahedron. Consequently, in the optimization of $LJ_{310-561}$ clusters, 297 and 147 atoms are fixed on the inner icosahedron without vertices and the inner Ino's decahedron, respectively. The remaining atoms are distributed randomly on the other lattice sites.

3. Results and Discussion

3.1. Validation of the Proposed Method. The proposed method based on the constructed lattices and genetic algorithm is validated by optimization of LJ_{13-309} clusters with icosahedral, decahedral, and truncated octahedral motifs. Results show that the proposed method successfully found all the lowest known minima. Optimization results of some LJ clusters that are generally known as very difficult cases are shown in Table 1.

TABLE 1: Energies and the Mean Optimization Time of Several Lennard-Jones Clusters

motif[a]	*N*	mean time (s)	succ/runs[b]	energy (ϵ)	motif	*N*	mean time (s)	succ/runs	energy (ϵ)
OCT	38	0.04252	50/50	−173.928 427		192	1.0206	50/50	−1175.697 143
FC	70	0.3823	50/50	−366.892 251		236	48.1858	47/50	−1480.034 326
	159	1.2547	50/50	−951.091 036		238	2.2425	50/50	−1494.438 246
	178	4.2150	50/50	−1079.083 854	IC	88	1.8053	49/50	−479.032 630
DEC	75	0.6076	50/50	−397.492 331		113	4.9660	47/50	−641.794 701
	77	0.5721	50/50	−409.083 516		115	8.7086	44/50	−655.756 305
	102	0.3377	50/50	−569.363 650		169	32.2235	15/50	−1017.611 215
	103	0.2183	50/50	−575.766 130		170	30.3858	17/50	−1024.791 797
	104	0.3295	50/50	−582.086 641		186	7.5346	50/50	−1132.669 966
	189	1.3474	50/50	−1153.637 014		187	7.8091	50/50	−1139.455 696

[a] Motifs OCT, FC, DEC, and IC are the truncated octahedron, anti-Mackay icosahedron, Marks' decahedron, and the Mackay icosahedron, respectively. [b] succ/runs means the number of successful runs out of the total runs.

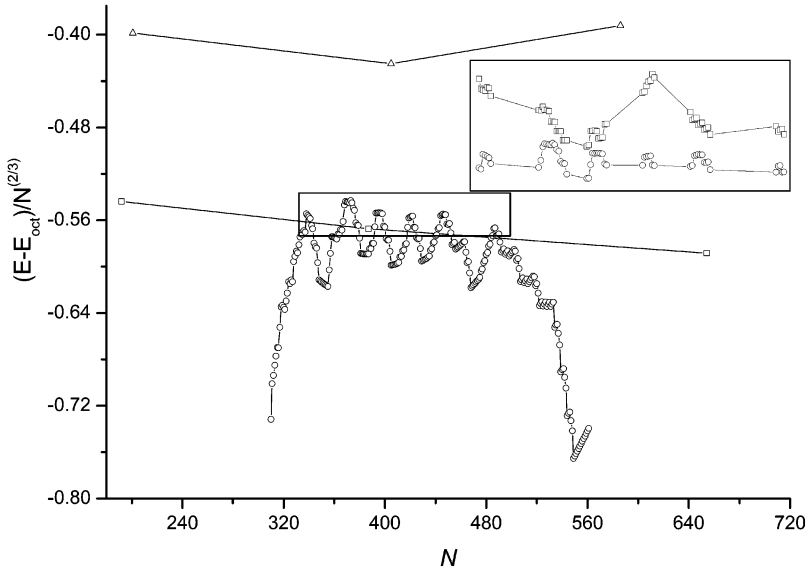

Figure 4. Energy comparison of the most stable truncated octahedral and Marks' decahedral sequence with the icosahedra: the truncated octahedron, Marks' decahedron, and the icosahedron are plotted with △, □, and ○, respectively. *N* is the number of atoms, *E* is the energy of the cluster with the icosahedron, Marks' decahedron, and the truncated octahedron, and E_{oct} is the fitting energy of the cuboctahedra.

From the Table 1, it can be found that all the energies are in agreement with published results.[35,36] This indicates that the proposed method based on the constructed lattices and the GA is reliable. The mean optimization time to find the global minimum for the LJ_{75} based on Ino's decahedral lattice containing 147 sites is around 0.6076 s (Pentium III, 1 GHz), while the mean time by a global optimization method is around 16.7 min (Pentium II, 333 MHz).[37] It is evident that the optimization time is shortened significantly. Moreover, the success ratio of 100% (50 out of 50) is higher than that of 5.4% in ref 37. Therefore, the proposed method is a great improvement in the optimization of LJ clusters, especially for clusters with Marks' decahedral and the truncated octahedral configurations because reasonable initial configurations can be generated based on constructed lattices. However, although the proposed method is highly efficient, it cannot find new configurations except for the icosahedral, decahedral, and truncated octahedral motifs because it is a modeling-based optimization method.

3.2. Putative Structures with Global Minima for $LJ_{310-561}$ Clusters. All the clusters in the range $309 < N \leq 561$ are optimized with the method. According to previous works, icosahedral configurations are predominant when the size is less than 1600.[15] Therefore, all the $LJ_{310-561}$ clusters are first optimized based on the icosahedral lattice. Putative lowest energies with icosahedral configurations are listed in Table 2.

In order to ascertain whether Marks' decahedral or the truncated octahedral configurations exist in $LJ_{310-561}$ clusters, the energies of the icosahedra, as listed in Table 2, are compared with the most stable sequences of the truncated octahedron and Marks' decahedron. The comparison is given in Figure 4. Energies of clusters are plotted as $(E - E_{oct})/N^{2/3}$ versus *N*, where *E* is the energy of Marks' decahedron, the truncated octahedron, and the icosahedron, and E_{oct} is the four-term least-squares fit to the binding energies of face-centered cubic (fcc) cuboctahedra.[38] In Figure 4, the line with the triangles is the most stable energy sequence of the octahedron, which can be obtained by comparing the energies of the regular truncated octahedra and the other truncated octahedra without regular hexagonal faces.[39] The line with the squares is the energetically most stable sequence of Marks' decahedron, which was reported in ref 27.

From Figure 4, it can be found that the Lennard-Jones clusters in the range $309 < N \leq 561$ with the truncated octahedral motif are not favorable because the line of the icosahedral energy always lies below that of the lowest energy sequence of the truncated octahedron. But the clusters in the rectangle above the line of the Marks' decahedral sequence may be Marks' decahedral configurations. Therefore, they are also optimized based on Ino's decahedral lattice. A comparison between the energies of Marks' decahedra and the icosahedra is shown in

TABLE 2: Lowest Icosahedral Energies (E) of $LJ_{310-561}$ Clusters

N^a	motif[b]	E^c (ϵ)	n^d	N	motif	E (ϵ)	n	N	motif	E (ϵ)	n	N	motif	E (ϵ)	n
310	FC	−2012.098 565	0	373	IC	−2455.261 852	5	436	IC	−2914.370 506	1	499	IC	−3375.440 662	0
311	IC	−2017.838 110	0	374	IC	−2462. 567 918	4	437	IC	−2921.599 324	0	500[e]	IC	−3382.693 487	0
312	IC	−2024.652 123	0	375	IC	−2470.032 175	5	438	IC	−2928.593 271	1	501	IC	−3389.946 441	0
313	IC	−2031.396 713	0	376	IC	−2477.339 088	4	439	IC	−2935.822 327	0	502	IC	−3397.196 422	0
314	IC	−2038.173 131	0	377	IC	−2485.115 011	5	440	IC	−2942.814 971	1	503	IC	−3404.627 600	0
315	IC	−2044.980 920	0	378	IC	−2492.443 691	4	441	IC	−2950.044 086	1	504	IC	−3412.477 434	0
316	FC	−2052.140 774	0	379	IC	−2499.684 891	4	442	IC	−2957.035 985	1	505	IC	−3419.730 528	0
317	FC	−2058.468 188	0	380	IC	−2507.480 023	5	443	IC	−2964.265 503	0	506	IC	−3427.621 193	0
318	FC	−2064.797 071	0	381	IC	−2515.387 833	4	444	IC	−2970.965 828	1	507	IC	−3435.687 722	0
319	IC	−2071.874 428	2	382	IC	−2522.629 194	4	445	IC	−2978.214 367	1	508	IC	−3442.940 773	0
320	IC	−2079.108 659	1	383	IC	−2529.870 662	4	446	IC	−2985.461 112	1	509	IC	−3450.193 949	0
321	IC	−2086.343 410	0	384	IC	−2537.103 074	3	447	IC	−2992.783 729	2	510	IC	−3457.807 978	0
322	IC	−2093.169 666	0	385	IC	−2544.335 413	2	448	IC	−3000.081 058	1	511	IC	−3465.061 048	0
323	IC	−2099.995 344	0	386	IC	−2551.565 720	1	449	IC	−3007.846 605	2	512	IC	−3472.314 244	0
324	FC	−2106.682 396	1	387	IC	−2558.796 497	0	450	IC	−3015.164 293	1	513	IC	−3479.926 793	0
325	FC	−2113.917 005	0	388	IC	−2565.793 770	1	451	IC	−3022.415 641	1	514	IC	−3487.179 880	0
326	FC	−2120.916 334	1	389	IC	−2573.024 522	0	452	IC	−3030.187 369	2	515	IC	−3494.433 094	0
327	FC	−2128.150 926	0	390	IC	−2580.021 240	1	453	IC	−3038.072 927	1	516	IC	−3501.685 912	0
328	FC	−2134.488 722	0	391	IC	−2587.251 965	0	454	IC	−3045.324 373	1	517	IC	−3508.938 736	0
329	IC	−2141.430 727	0	392	IC	−2593.731 432	0	455	IC	−3052.572 975	1	518	IC	−3516.340 448	0
330	IC	−2148.373 452	1	393	IC	−2600.322 076	3	456	IC	−3060.221 313	1	519	IC	−3524.193 917	0
331	IC	−2155.607 546	0	394	IC	−2607.564 869	3	457	IC	−3067.473 860	1	520	IC	−3531.446 857	0
332	IC	−2162.436 139	0	395	IC	−2614.796 092	2	458	IC	−3074.722 501	1	521	IC	−3539.331 418	0
333	FC	−2169.283 670	0	396	IC	−2622.026 782	1	459	IC	−3081.971 267	1	522	IC	−3547.397 239	0
334	FC	−2176.278 417	1	397	IC	−2629.283 637	4	460	IC	−3089.218 142	1	523	IC	−3554.650 103	0
335	FC	−2183.512 126	0	398	IC	−2636.566 153	3	461	IC	−3096.465 023	1	524	IC	−3561.903 096	0
336	FC	−2190.508 068	1	399	IC	−2644.371 470	4	462	IC	−3103.692 087	0	525	IC	−3569.515 910	0
337	FC	−2197.741 651	0	400	IC	−2651.675 335	3	463	IC	−3110.995 000	1	526	IC	−3576.768 781	0
338	IC	−2204.148 933	2	401	IC	−2659.459 309	4	464	IC	−3118.849 641	1	527	IC	−3584.021 780	0
339	IC	−2211.382 035	1	402	IC	−2666.784 339	3	465	IC	−3126.703 679	1	528	IC	−3591.632 543	0
340	IC	−2218.615 332	0	403	IC	−2674.029 018	3	466	IC	−3133.956 743	1	529	IC	−3598.885 418	0
341	IC	−2225.849 333	6	404	IC	−2681.814 373	4	467	IC	−3141.864 153	1	530	IC	−3606.138 371	0
342	IC	−2233.317 755	7	405	IC	−2689.713 734	3	468	IC	−3149.937 648	1	531	IC	−3613.747 101	0
343	IC	−2240.629 347	6	406	IC	−2696.958 552	3	469	IC	−3157.190 780	1	532	IC	−3620.999 928	0
344	IC	−2248.419 339	7	407	IC	−2704.203 470	3	470	IC	−3164.439 402	1	533	IC	−3628.252 883	0
345	IC	−2255.752 944	6	408	IC	−2711.448 516	3	471	IC	−3171.688 153	1	534	IC	−3637.063 978	0
346	IC	−2262.986 228	5	409	IC	−2718.677 721	2	472	IC	−3178.936 910	1	535	IC	−3644.316 423	0
347	IC	−2270.792 335	7	410	IC	−2725.907 421	1	473	IC	−3186.185 673	1	536	IC	−3651.645 144	0
348	IC	−2278.712 819	6	411	IC	−2733.137 599	0	474	IC	−3193.434 565	1	537	IC	−3659.528 247	0
349	IC	−2285.948 844	6	412	IC	−2740.133 627	1	475	IC	−3200.661 820	0	538	IC	−3667.569 346	0
350	IC	−2293.181 867	5	413	IC	−2747.363 766	0	476	IC	−3207.648 521	1	539	IC	−3676.488 957	0
351	IC	−2300.415 404	4	414	IC	−2754.359 151	1	477	IC	−3214.876 229	0	540	IC	−3683.741 345	0
352	IC	−2307.648 892	3	415	IC	−2761.589 267	0	478	IC	−3221.861 849	1	541	IC	−3691.070 873	0
353	IC	−2314.882 331	2	416	IC	−2768.583 569	1	479	IC	−3229.090 010	0	542	IC	−3698.954 026	0
354	IC	−2322.116 283	1	417	IC	−2775.814 036	0	480	IC	−3236.073 847	1	543	IC	−3706.947 842	0
355	IC	−2329.348 216	0	418	IC	−2782.294 090	0	481	IC	−3243.302 482	0	544	IC	−3715.921 820	0
356	IC	−2335.824 444	0	419	IC	−2789.103 123	2	482	IC	−3250.284 319	1	545	IC	−3723.174 136	0
357	IC	−2342.300 677	0	420	IC	−2796.332 973	1	483	IC	−3257.513 447	0	546	IC	−3730.504 075	0
358	IC	−2348.782 310	0	421	IC	−2803.561 840	0	484	IC	−3264.493 944	1	547	IC	−3738.387 886	0
359	IC	−2355.979 723	3	422	IC	−2810.822 287	2	485	IC	−3271.723 567	0	548	IC	−3746.370 707	0
360	IC	−2363.212 317	2	423	IC	−2818.620 347	3	486	IC	−3278.672 947	1	549	IC	−3755.363 288	0
361	IC	−2370.445 417	1	424	IC	−2825.919 312	2	487	IC	−3285.966 242	0	550	IC	−3762.615 484	0
362	IC	−2377.676 598	0	425	IC	−2833.695 861	3	488	IC	−3293.718 435	1	551	IC	−3769.867 806	0
363	IC	−2384.656 316	1	426	IC	−2841.015 818	2	489	IC	−3301.032 607	0	552	IC	−3777.120 251	0
364	IC	−2391.887 483	0	427	IC	−2848.263 899	2	490	IC	−3308.285 790	0	553	IC	−3784.372 705	0
365	IC	−2398.871 603	1	428	IC	−2856.041 341	3	491	IC	−3316. 048 882	1	554	IC	−3791.625 165	0
366	IC	−2406.102 769	0	429	IC	−2863.931 336	2	492	IC	−3323.927 687	0	555	IC	−3798.877 759	0
367	IC	−2412.9280 06	0	430	IC	−2871.179 553	2	493	IC	−3331.180 850	0	556	IC	−3806.130 231	0
368	IC	−2419.406 128	0	431	IC	−2878.427 881	2	494	IC	−3338.432 495	0	557	IC	−3813.382 820	0
369	IC	−2426.449 891	3	432	IC	−2885.673 325	2	495	IC	−3346.058 571	0	558	IC	−3820.635 415	0
370	IC	−2433.683 009	2	433	IC	−2892.918 777	2	496	IC	−3353.311 762	0	559	IC	−3827.888 029	0
371	IC	−2440.915 149	1	434	IC	−2900.147 182	1	497	IC	−3360.564 557	0	560	IC	−3835.140 761	0
372	IC	−2448.145 557	0	435	IC	−2907.376 080	0	498	IC	−3368.187 444	0	561	IC	−3842.393 626	0

[a] N_{atom} is the atom number of the LJ cluster. [b] Motif is IC (Mackay icosahedron) or FC (anti-Mackay icosahedron). [c] E is the putative global minima. [d] n is the number of missing atoms in the icosahedral core. [e] The potential value was reported in ref 37.

the enlarged graph shown in the inset. From the enlarged graph, it can be found that Marks' decahedral configurations are not favorable. Therefore, from the above analysis, it is clear that all the Lennard-Jones clusters in the range $309 < N \leq 561$ are icosahedral motifs, which is consistent with the conclusion given by Farges.[40]

3.3. The Structural Characters of $LJ_{310-561}$. From the number of missing atoms in the icosahedral core, n, listed in Table 2, it can be found that the structures with an incomplete core in the range of $309 < N \leq 561$ occupy a high proportion, although the core of clusters with $N > 491$ is full. Moreover, the number of missing atoms goes to seven in LJ_{342}, LJ_{344}, and

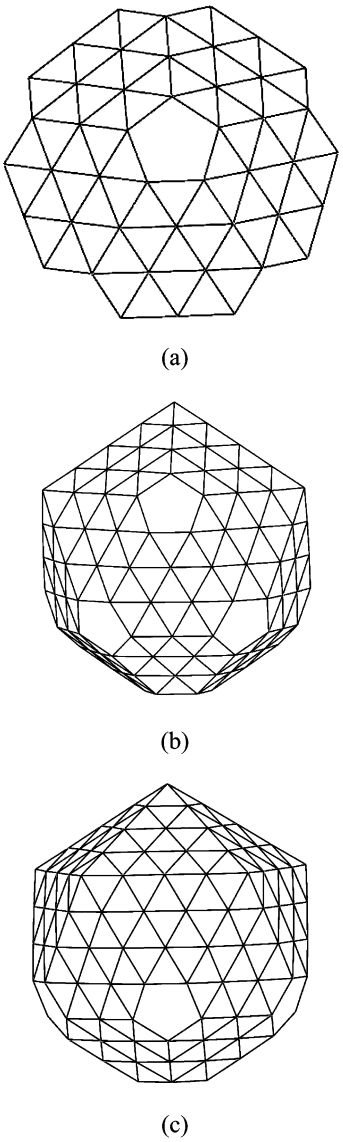

Figure 5. Configurations of the fifth and fourth shells of LJ_{347}. (a) The planform of the fifth shell. (b) The front of the fourth shell. (c) The back of the fourth shell.

LJ_{347}. The structure of LJ_{347} is shown in Figure 5. The atoms on the outermost shell, as shown in Figure 5a, form a highly symmetric configuration and cap the fourth shell. The vacant sites, as shown in Figure 5b and c, are far from the region where the atoms of the outermost shell lump together. These structural characters had been observed in LJ clusters with atoms less than 309.[24,34]

From the motif listed in Table 2, it can also be found that $LJ_{310-561}$ clusters prefer FC configurations when the atoms on the outermost shell are fewer because FC sites are more strongly bound to the core. The intershell interaction is the dominant contribution to the energy of clusters. With the increase in the number of atoms on the outermost shell, the intrashell interaction becomes important; the favored structures of the clusters shift to the IC configurations because the IC lattice has a higher surface density than that of the FC lattice.[22] The proportion of FC and IC configurations in the range of $309 < N \leq 561$ is calculated and tabulated in Table 3. In order to understand the structural distribution of FC and IC in the range of $309 < N \leq 561$, the results of the former shells are also given. From Table 3, it can be found that the proportion of FC configurations decreases with increasing number of shells, while IC increases.

TABLE 3: Structural Distribution of FC and IC[a]

n	atom range	N_n	N_{fc}	N_{ic}	N_{ic}/N_n	N_{fc}/N_n
2	13−55	42	17	24	0.571	0.405
3	56−147	92	23	63	0.685	0.250
4	148−309	162	19	135	0.833	0.117
5	310−561	252	14	238	0.944	0.056

[a] n is the number of the icosahedral shell; N_n is the number of sites on the nth shell; N_{fc} and N_{ic} are the number of configurations with FC and IC in each shell.

The reason may be the fact that the intrashell interaction gets more and more important as the lattice sites increase.

4. Conclusion

Geometric methods for the construction of three structural motifs, the icosahedron, Ino's decahedron, and the complete octahedron, are proposed. On the basis of constructed lattices and the genetic algorithm, a global optimization method for large Lennard-Jones clusters is presented and applied to the global optimization of Lennard-Jones clusters. It was shown that the proposed method is highly efficient, and it is a good tool for optimization of large size LJ clusters. With the algorithm, the putative global minima of $LJ_{310-561}$ clusters are predicted. By comparison of the optimization results and analysis of the structures of the LJ clusters, it is shown that all the $LJ_{310-561}$ clusters are icosahedral motifs, and the structures with an incomplete core occupy a high proportion. Moreover, the proportion of FC configurations in the range $309 < N \leq 561$ is low compared with that of the former shells; but further verification or proof is still needed.

Acknowledgment. This study is supported by the Teaching and Research Award Program for Outstanding Young Teachers (TRAPOYT) in higher education institutions of the Ministry of Education (MOE), P. R. China and the outstanding youth fund (No. 20325517) from the National Natural Scientific Foundation of China (NNSFC).

References and Notes

(1) Wales, D. J.; Scheraga, H. A. *Science* **1999**, *285*, 1368−1372.
(2) Hoare, M. R. *Adv. Chem. Phys.* **1979**, *40*, 49−135.
(3) Deaven, D. M.; Ho, K. M. *Phys. Rev. Lett.* **1995**, *75*, 288−291.
(4) Deaven, D. M.; Tit, N.; Morris, J. R.; Ho, K. M. *Chem. Phys. Lett.* **1996**, *256*, 195−200.
(5) . Wolf, M. D.; Landman, U. *J. Phys. Chem. A*, **1998**, *102*, 6129−6137.
(6) Wille, L. T. *Chem. Phys. Lett.* **1987**, *133*, 405−410.
(7) Ma, J.; Straub, J. E. *J. Chem. Phys.* **1994**, *101*, 533−541.
(8) Xue, G. *J. Global Optim.* **1994**, *4*, 187−208.
(9) Schelstraete, S.; Verschelde, H. *J. Phys. Chem. A* **1997**, *101*, 310−315.
(10) Cai, W. S.; Jiang, H. Y.; Shao, X. G. *J. Chem. Inf. Comput. Sci.* **2002**, *42*, 1099−1103.
(11) Wales, D. J.; Doye, J. P. K. *J. Phys. Chem. A* **1997**, *101*, 5111−5116.
(12) Cai, W. S.; Shao, X. G. *J. Comput. Chem.* **2002**, *23*, 427−435.
(13) Cai, W. S.; Feng, Y.; Shao, X. G.; Pan, Z. X. *J. Mol. Struct.: THEOCHEM* **2002**, *579*, 229−235.
(14) Jiang, H. Y.; Cai, W. S.; Shao, X. G. *Phys. Chem. Chem. Phys.* **2002**, *4*, 4782−4788.
(15) Raoult, B.; Farges, J.; De Feraudy, M. F.; Torchet, G. *Philos. Mag. B***1989**, *60*, 881−906.
(16) Doye, J. P. K.; Calvo, F. *J. Chem. Phys.* **2002**, *116*, 8307−8317.
(17) Van de Waal, B. W. *J. Chem. Phys.* **1993**, *98*, 4909−4919.
(18) Cleveland, C. L.; Landman, U. *J. Chem. Phys.* **1991**, *94*, 7376−7396.
(19) Besley, N. A.; Johnston, R. L.; Stace, A. J.; Uppenbrink, J. *J. Mol. Struct.: THEOCHEM* **1995**, *341*, 75−90.
(20) Doye, J. P. K.; Wales, D. J. *Chem. Phys. Lett.* **1995**, *247*, 339−347.

(21) Hearn, J. E.; Johnston, R. L. *J. Chem. Phys.* **1997**, *107*, 4674−4687.
(22) Northby, J. A. *J. Chem. Phys.* **1987**, *87*, 6166−6177.
(23) Xue, G. L. *J. Global Optim.* **1994**, *4*, 425−440.
(24) Romero, D.; Barron, C.; Gomez, S. *Comput. Phys. Commun.* **1999**, *123*, 87−96.
(25) Leary, R. H.; Doye, J. P. K. *Phys. Rev. E* **1999**, *60*, R6320−R6322.
(26) Hendy, S. C.; Doye, J. P. K. *Phys. Rev. B* **2002**, *66*, 235402(1−8).
(27) Jiang, H. Y.; Cai, W. S.; Shao, X. G. *J. Phys. Chem. A* **2003**, *107*, 4238−4243.
(28) Liu, D. C.; Nocedal, J. *Math. Progm.* **1989**, *45*, 503−528.
(29) Betts, S.; Browne, S.; Dongarra, J.; Grosse, E.; McMahan, P.; Rowan, T. Netlib Repository at UTK and ORNL. http://www.netlib.org.
(30) Kabrede, H.; Hentschke, R. *J. Phys. Chem. B* **2003**, *107*, 3914−3920.
(31) Hartke, B. *Chem. Phys. Lett.* **1995**, *240*, 560−565.
(32) Niesse, J. A.; Mayne, H. R. *J. Comput. Chem.* **1997**, *18*, 1233−1244.
(33) Johnston, R. L. *Dalton Trans.* **2003**, *22*, 4193−4207.
(34) Barron, C.; Gomez, S.; Romero, D. *Appl. Math. Lett.* **1997**, *10*, 25−28.
(35) Lennard-Jones Clusters. http://www-wales.ch.cam.ac.uk/∼jon/structures/LJ.html.
(36) University of Houston, Cluster with Minimum LJ potential. http://ithaki.vcl.uh.edu/∼cbarron/LJ_cluster/LJpottable.html.
(37) Krivov, S. V. *Phys. Rev. E* **2002**, *66*, R025701(1−4).
(38) Xie, J.; Northby, J. A.; Freeman, D. L.; Doll J. D. *J. Chem. Phys.* **1989**, *91*, 612−619.
(39) Doye, J. P. K.; Wales, D. J. *Chem. Phys. Lett.* **1996**, *262*, 167−174.
(40) Farges, J.; De Feraudy, M. F.; Raoult, B.; Torchet, G. *J. Chem. Phys.* **1986**, *84*, 3491−3501.